

**UNIQUE CONSIDERATIONS IN THE
DESIGN AND EXPERIMENTAL
EVALUATION OF TAILORED WINGS WITH
ELASTICALLY PRODUCED CHORDWISE CAMBER**

**Lawrence W. Rehfield, Peter J. Zischka,
Michael L. Fentress and Stephen Chang**

University of California, Davis

516-24

51384

P18

SUMMARY

In this paper, some of the unique considerations that are associated with the design and experimental evaluation of chordwise deformable wing structures are addressed. Since chordwise elastic camber deformations are desired and must be free to develop, traditional rib concepts and experimental methodology cannot be used. New rib design concepts are presented and discussed. An experimental methodology based upon the use of a flexible sling support and load application system has been created and utilized to evaluate a model box beam experimentally.

Experimental data correlate extremely well with design analysis predictions based upon a beam model for the global properties of camber compliance and spanwise bending compliance. Local strain measurements exhibit trends in agreement with intuition and theory but depart slightly from theoretical perfection based upon beam-like behavior alone. It is conjectured that some additional refinement of experimental technique is needed to explain or eliminate these (minor) departures from asymmetric behavior of upper and lower box cover strains. Overall, a solid basis for the design of box structures based upon the bending method of elastic camber production has been confirmed by the experiments.

INTRODUCTION

Elastic tailoring refers to the utilization of the design flexibility of composites to achieve performance goals. The goals are usually accomplished by selecting an appropriate structural concept, fiber orientation, ply stacking sequence and a blend of materials. In aeronautical applications, emphasis has been given to tailoring deformations which influence the aerodynamics of the system (ref. 1). This is called "aeroelastic tailoring." Aeroelastic instabilities may be avoided in this manner (ref. 1), as in the X-29, or performance enhancements, such as increased lift (refs. 2, 3) or maximizing lift-to-drag ratio (ref. 1), can be achieved.

Early work in aeroelastic tailoring focused on simple laminated construction of plate-like, rather low aspect ratio lifting surfaces. The design procedures are described in ref. 4 in the following manner:

"The design for a desired static aeroelastic response was initially an iterative process performed by a structural engineer trying to satisfy a requirement for twist and camber established by an aerodynamicist."

Since that time, considerable progress has been made, including the effective use of optimization algorithms (refs. 1,4). Emphasis, however, seems to have been given always to tailoring specific configurations to specific missions, a practice that did not foster scientific understanding or permit a firm grasp of the cause-effect relationship between configuration and response. In contrast to this approach, our research breaks with the past and focuses upon understanding, modeling, tailoring mechanisms and creating design concepts that accentuate individual behavioral characteristics.

Interest in swept forward wings, which resulted in the X-29, focused attention on wing bending and twisting deformations. As these deformation modes are understood rather well now, our research has emphasized elastically produced chordwise camber. While camber deformations have been tailored by ad hoc methods for specific configurations (ref. 4), it remained to create the basis for scientific understanding of behavior and design concepts which accentuate this deformation mode.

Structural tailoring concepts have been developed to create wings with elastically produced camber for the purpose of increasing the lift generated by the wing. Currently, the usual means of accomplishing this is with controls, the most common of which are flaps. If natural, intrinsic means are used to enhance lift, then flap requirements and their associated systems may be reduced. This will yield weight savings, acquisition cost savings and maintenance cost savings. The desired effects are presented in figure 1.

The fundamental mechanisms that are utilized produce camber deformations in response to the usual loading of the wing such as bending moments and torque. The camber enhances the production of lift and further modifies the loads. Significant lift increases may be produced by tailoring using modern composite material systems (refs. 2,3). An overview of this research is given in ref. 2.

There are several general concepts that have been used in our tailoring work. They are illustrated in figures 2 and 3. The continuous filament grid stiffened structures (figure 3) are particularly useful for tailoring response.

In this paper, we address two issues that are unique to chordwise deformable wings. Since chordwise elastic camber deformations are desired and must be free to develop, traditional rib concepts and experimental methodology cannot be used. We present and discuss new rib design concepts and an experimental methodology based upon the use of a flexible sling support and load application system. Experimental data are shown to be in excellent agreement with design analysis predictions for the bending method of producing elastic chordwise camber.

The cornerstone of elastic tailoring with composites is modeling. We selected the well established thin-walled beam theory (refs. 5-7) to serve as a basis for our models of high aspect ratio wings, appropriately modified to predict chordwise camber deformations (refs. 2,3). An established body of knowledge appears in refs. (2,3,8-12). Of particular importance is the correlation shown between the beam model and extensive finite element simulations for the bending case (refs. 8,12).

RIB CONCEPTS FOR CHORDWISE DEFORMABLE WINGS

Along with the development of elastically tailored chordwise deformable wings, it is necessary to design a compatible rib structure that allows the chordwise deformation to occur while still performing some of the traditional functions of a rib. A traditional rib is designed to: 1) preserve the cross section geometry, 2) distribute pressure loads to the spars and stiffeners, 3) support the wing covers, and 4) serve as attachment locations for system equipment. The new chordwise deformable rib still transfers pressure loads and provides cover support, but it must allow the cross section geometry to camber. Five new rib design concepts appear in figures 4-8.

Figure 4 shows the Vertical Column Support type of rib structure. This style of rib is attractive because it is easily joined to the proposed grid stiffening structure of the wing box (refs. 2,3,8-10). Due to the method of constructing the grid structure, convenient points of attachment for the columns are created. To minimize the restraint of the rib on chordwise deformation, it is proposed to use universal joints to attach the columns to the grid. The grid structure needs to be sized such that the columns can be placed at the proper spanwise intervals so that they support the covers against general instability buckling modes.

The Accordion Rib, unlike the column supports, provides continuous chordwise support to the covers while still allowing differential expansion of the upper and lower structural wing box covers. The Accordion Rib looks much like the pleated portion of an accordion. The pleats will conform to the grid structure as shown in figure 5.

The Diagonal Rib Structures, figures 6 and 7, consist of diagonal columns fastened to the grid structure like the Vertical Columns via universal joints. Figure 6 shows the Segmented Diagonal Columns jointed at their intersection while figure 7, Crossed Diagonal Columns, shows no midsection joint.

The Floating Rib Structure, figure 8, is constructed of crossed diagonal ribs with one end fastened with a universal joint and the other free to float. The floating end rests on an abrasion pad that attaches to the upper and lower wing covers.

A detailed design analysis is required for sizing the individual elements in these configurations. These suggestions should prove useful as technology for chordwise deformable wings advances.

EXPERIMENTAL METHODOLOGY

Attention is restricted to the bending method (refs. 2,3,8-10,12) of creating elastically produced chordwise camber deformation. This method produces an intentionally exaggerated form of anticlastic chordwise curvature, which is a natural tendency in response to spanwise bending. The key to successfully using this approach is to create large effective Poisson's ratios in the wing box covers while preserving the essential integrity of the box cross section.

The "best" test to perform in order to evaluate and validate camber production experimentally is a four-point bending test. This test method creates a gage section in the specimen that is exposed to a pure spanwise bending moment only, a simple state of loading that isolates the desired effect of anticlastic curvature. The challenge, of course, is to create a way of performing the test that utilizes methods of load application and support that permit chordwise camber deformations to freely occur.

Test Specimen Design

The box beam test specimen (figure 9) has been designed with three factors in mind. First, due to the dimensions of our PHI laminating press, the box covers are limited to a maximum length of twenty inches. The cover layup is taken to be $[\pm 26]$ in keeping with our optimized design without stiffeners (refs. 2,3,12). Second, to prevent the covers from buckling under the four point bending loading, a cover width of four inches and a thickness of twelve plies has been selected. This also is in concert with the third factor, which is to produce easily measurable strain levels.

To prevent the covers from buckling, it is necessary to predict the buckling load of the box beam covers. The bending stiffness of the beam was determined using the cross sectional geometry of the box and material properties of the laminate and aluminum channel. Two methods have been used to calculate the buckling load of the box covers and the results compare well with each other. The properties of AS4/3501-6 graphite-epoxy have been used in the design analysis (refs. 2,3,12) for the covers.

The first method used was to derive the buckling equations for an orthotropic plate with two fixed opposing ends and two simply supported opposing ends. A closed form solution for a buckling problem with these boundary conditions does not exist, so the commercially available numerical solution program "Theorist" was used to solve for the determinant of the buckling equation. This solution yields a buckling load of 1,016 lbs, which in turn relates to a strain level of $1,565\mu \epsilon$. The second method used was to

determine the ratio of buckling loads for a simply supported isotropic plate to that of a fixed-fixed, simply supported isotropic plate with the same aspect ratio. This factor was then used to determine the buckling load of the orthotropic fixed-fixed simply supported plate from that of a simply supported on all sides orthotropic plate. The resulting buckling load and strain level were determined to be 1,102 lbs. and 1,701 $\mu\epsilon$, respectively. Thus, in view of the approximate nature of the second method, the results compare rather well.

Experimental Methodology

A number of possible approaches for performing the four-point bending tests were devised and thoroughly evaluated. With the help of Dr. Damodar Ambur of the NASA Langley Research Center, the "Sling Supported Method" was selected for implementation. Figure 10 illustrates this approach in schematic form. An attractive feature of this method is the fact that the entire assembly is placed in the hydraulic grips of our 75 kip MTS universal testing machine and pulled in tension. The flexible slings of nylon strap material are used to both support the test specimen and apply the four-point loading. This concept would seem to provide minimal resistance to the elastically produced camber deformations.

In addition to testing the wing box, a series of component and coupon tests and a detailed finite element analysis of the fixtures were performed. Measured property data on coupon tests were used for correlating the test results with theory in the second method of camber correlation, which is discussed subsequently.

All specimen response measurements were made with resistance strain gages. While displacement measurements would have been useful, the floating nature of the test setup makes them extremely inconvenient and potentially unreliable. A diagram showing the strain gage nomenclature and locations appears in figure 11.

RESULTS AND DISCUSSION

Basic Strain Gage Data

Strain gage data appear in figures 12-14 as functions of applied bending moment. Figure 12 shows data from the chordwise strain gages. The zero reference line is provided because, in a theoretically perfect test, the top and bottom gage readings should be symmetrically located about this reference line.

Data from the two spanwise centrally located gages appear in figure 13. Again the zero reference line is provided. Ideally, the two gages should read the opposite of each other.

Data from the two outer or remote spanwise gages mounted on the bottom surface are presented in figure 14. These data were used, together with turnbuckle adjustments, to balance out the load application system with a small amount of preload applied. Theoretically, if the test conditions were ideal, the data from these two gages would be identical. This would correspond to perfect four-point bending conditions.

The above test results suggest that the objectives of the experiment were met, and the behavior reflected is as anticipated. They must be regarded as preliminary, however, as we believe that a further developed testing technique may produce results in closer agreement with "theoretical perfection."

Of particular interest is the ability of the structure to produce global chordwise camber curvature. This capability was optimized for the box covers with the $[\pm 26]$ ply layup for AS4/3501-6 graphite-epoxy (refs. 2,3,12). Several basic relations are needed to interpret the measured data.

Elementary Mechanics Model

The first relationship involves the spanwise curvature and membrane strains in the box. Let "1" denote the spanwise direction and "2" the normal chordwise direction. If the usual Bernoulli-Euler assumption, which is valid under pure bending, is adopted, we can write

$$\kappa_{11} = \text{Spanwise Curvature} = (\epsilon_{11}^l - \epsilon_{11}^u) / (H+h) \quad (1)$$

where κ_{11} is the spanwise curvature, ϵ_{11} is the spanwise membrane extensional strain, H is the thickness or depth of the box, h is the cover thickness and the subscripts "l" and "u" refer to the lower and upper covers of the box, respectively.

The second relation provides the elastic law relating spanwise curvature and bending moment. It is, in the notation of ref. 5,

$$\kappa_{11} = S_{55} M_y \quad (2)$$

The spanwise bending moment is M_y , and S_{55} is the spanwise bending compliance. It is related to the stiffness, C_{55} , as follows (ref. 5):

$$S_{55} = (C_{55})^{-1} \quad (3)$$

and

$$\begin{aligned} C_{55} &= \text{Spanwise Bending Stiffness} \\ &= 2c_s K_{11} \left(\frac{H}{2}\right)^2 + 2(EI)_c \end{aligned} \quad (4)$$

In equation (4), c_s denotes the structural chord or width of the box. $(EI)_c$ is the bending stiffness of the aluminum closure channel (figure 9) about a chordwise parallel axis, and K_{11} is the spanwise extensional stiffness of the box covers. It is shown in ref. 5 that

$$K_{11} = A_{11} - (A_{12})^2 / A_{22} \quad (5)$$

where the A_{ij} ($i, j = 1, 2, 6$) are membrane stiffnesses from lamination theory.

For balanced cover configurations and uniaxial stress conditions (ref. 5)

$$\epsilon_{22} = - (A_{12} / A_{22}) \epsilon_{11} \quad (6)$$

The ratio (A_{12} / A_{22}) is an effective Poisson ratio for the laminated covers.

From classical Bernoulli-Euler bending theory

$$\begin{aligned} \kappa_{22} &\equiv \kappa_c, \text{ the Camber Curvature} \\ &= (A_{12} / A_{22}) \kappa_{11} \end{aligned} \quad (7a)$$

$$= (A_{12} / A_{22}) S_{55} M_y \quad (7b)$$

$$= (\epsilon_{22}^u - \epsilon_{22}^l) / (H+h) \quad (7c)$$

Eq. (7c) is analogous to eq. (1), and ϵ_{22} is the chordwise extensional membrane strain. Consequently, we define the camber bending compliance such that

$$\kappa_c = S_{cs} M_y \quad (8)$$

and the camber compliance is

$$S_{cs} = (A_{12}/A_{22}) S_{55} \quad (9)$$

Camber Correlation

The most desirable way to correlate theory and experiment is to use measured properties on the actual test specimen itself in the theoretical calculations. This is because there is batch-to-batch variation in composite materials themselves and some amount of variation from part-to-part due to processing. This is normal for composite structures and is accounted for in design by the allowable properties that are used in the design analysis. Our purposes here, however, are to evaluate (1) actual versus theoretical elastic camber production, (2) the suitability of the test methodology and (3) the validity of the model that has been created for use in design analysis. With these objectives in mind, our correlation study proceeded in a direct manner along two paths.

The first path or method is based upon using the experimentally determined spanwise bending compliance as the primary cover load-bearing elastic characteristic. This compliance is readily determined from the plot of experimental data shown in figure 15. This figure is based upon the use of eqs. (1) and (2). The measured spanwise bending compliance, S_{55} , together with the theoretical value of the effective Poisson ratio of 1.26 (refs. 2,3) and eq. (9), permits an estimate of the camber compliance to be calculated. This value is compared with the experimentally determined one obtained from figure 16 in table 1. The "experimental" value is based upon eqs. (7c) and (8).

While the agreement reflected in table 1 is excellent, another way of interpreting this information is that (A_{12}/A_{22}) can be found experimentally from measured compliances (figures 15,16) and eq. (9). This yields an effective Poisson ratio of 1.27, which is in good agreement with the value assumed in the design analysis (1.26). If the cover spanwise membrane stiffness K_{11} is back calculated from the experimentally determined spanwise bending compliance, known dimensions and properties of the closure channels, a value of 0.41×10^6 lb/in is obtained.

The second path or method utilizes a completely theoretical calculation with a value of K_{11} of 0.52×10^6 lb/in obtained from the test of a coupon specimen from another $[\pm 26]_{3s}$ laminate. The correlation of spanwise bending compliance appears in table 2. Camber compliance correlation is presented in table 3. Agreement is considered quite good by this method, so this data, together with that of table 1, confirms that the box beam behaves in a global manner consistent with the beam-like model of ref. 5.

CONCLUDING REMARKS

In this paper, we have addressed the unique considerations that are associated with the design and experimental evaluation of chordwise deformable wing structures. Since chordwise elastic camber deformations are desired and must be free to develop, traditional rib concepts and experimental methodology cannot be used. New rib design concepts are presented and discussed. An experimental methodology based upon the use of a flexible sling support and load application system has been created and utilized to evaluate a model box beam experimentally.

Experimental data correlates extremely well with design analysis predictions based upon a beam-like model for the global properties of camber compliance and spanwise bending compliance. Local strain measurements exhibit trends in agreement with intuition but which depart slightly from theoretical perfection in terms of upper and lower cover asymmetry. Additional work on the experiment technique is needed to help establish the cause for this (minor) departure from beam-like local behavior. Overall, a solid basis for the design of box structures based upon the bending method of elastic camber production has been confirmed by the experiments.

We wish to record our frustration at a drawback to experimental composite structures research in a university environment. Needed materials are required only in small quantities and are, therefore, difficult to obtain if prudent resource management is exercised. For example, our original test specimen design was based upon the use of standard aluminum channels that are 0.75 inches high and composite covers made of AS4/3501-6 graphite-epoxy unidirectional tape. Unfortunately, because AS4/3501-6 material is used in current aircraft production programs (which is the reason that we selected it), we were unable to obtain it in a timely manner and in a suitable quantity. Also, the desired aluminum channel stock was not available in Northern California. As a consequence, substitutions were made. The unfortunate result is that the extensive finite element correlation study results reported in refs. 3 and 12 cannot be compared directly to our experimental findings.

Since the agreement between finite element simulations and the beam-like predictions was excellent (refs. 3,12) in the earlier studies and the correlation with experiments is very good here, we consider that the design of high aspect chordwise deformable wings by utilizing the bending method of producing camber is on firm ground. Nevertheless, we are somewhat frustrated by the circumstances.

ACKNOWLEDGMENTS

This research was sponsored by the NASA Langley Research Center under Advanced Composites Technology Program Contract NAS1-18754. This support is gratefully acknowledged. A particular debt is owed to Dr. Damodar R. Ambur, the NASA Project Engineer, for his help with the development of the experimental methodology and his wise counsel. In addition, we thank Dr. T. J. Petersen of the Boeing Commercial Airplane Group for supplying us with the composite material, which was Fortafil 3(c)/8601 graphite-epoxy unidirectional tape.

REFERENCES

1. Shirk, M.H., Hertz, T.J. and Weisshaar, T.A., "A Survey of Aeroelastic Tailoring-Theory, Practice, Promise," Journal of Aircraft, Vol. 23, No. 1, January 1986, pp. 6-18.
2. Rehfield, L.W., Chang, S., Pickings, R.D., Zischka, P.J. and Holl, M.W., "Tailored Composite Wings With Elastically Produced Chordwise Camber," NASA Conference Publication 3104, Part 2, 1991, pp. 1037-1047.
3. Rehfield, L.W., Chang, S., Zischka, P.J., Pickings, R.D. and Holl, M.W., "Tailoring of Composite Wing Structures for Elastically Produced Camber Deformations," AIAA Paper No. 91-1186, Proceedings of the 32nd AIAA Structures, Structural Dynamics and Materials Conference, April 8-10, 1991, Baltimore, MD, Part 3, pp. 2123-2127.
4. Rogers, W.A., Braymen, W.W. and Shirk, M.H., "Design, Analysis, and Model Tests of an Aeroelastically Tailored Lifting Surface," AIAA Paper No. 81-1673, AIAA Aircraft Systems and Technology Conference, August 11-13, 1981, Dayton, OH.
5. Rehfield, L.W., "Design Analysis Methodology for Composite Rotor Blades," Proceedings of the Seventh DoD/NASA Conference on Fibrous Composites in Structural Design, AFWAL-TR-85-3094, June 1985, pp. (V(a)-1)-(V(a)-15).
6. Rehfield, L.W., Hodges, D.H., and Atilgan, A.R., "Nonclassical Behavior of Thin-Walled Beams with Closed Cross Sections," Journal of the American Helicopter Society, Vol. 35, No. 2, April 1990, pp. 42-50.
7. Rehfield, L.W. and Atilgan, A.R., "Toward Understanding the Tailoring Mechanisms for Thin-Walled Composites Tubular Beams," Proceedings of the First USSR-US Symposium on Mechanics of Composite Materials, 23-25 May 1989, Riga, Latvia, USSR, ASME, pp. 187-196.
8. Rehfield, L.W., Pickings, R.D., Chang, S. and Holl, M.W., "A Comparison of Classical Mechanics Models and Finite Element Simulation of Elastically Tailored Wing Boxes," NASA Conference Publication 3104, Part 2, pp. 809-816.
9. Ambur, D.R. and Rehfield, L.W., "Effect of Stiffness Characteristics on the Response of Composite Grid-Stiffened Structures," AIAA Paper No. 91-1087, Proceedings of the 32nd AIAA Structures, Structural Dynamics and Materials Conference, April 8-10, 1991, Baltimore, MD, Part 2, pp. 1349-1356.
10. Rehfield, L.W., Chang, S. and Atilgan, A.R., "New, Unusual and Nonclassical Behavior of Thin-Walled Composite Structures," Eighth International Conference on Composite Materials, Honolulu, HI, July 15-19, 1991, Composites: Design, Manufacture and Application, S.W. Tsai and G.S. Springer, editors, SAMPE, 1991, (26-A-1)-(26-A-9).
11. Zischka, P.J., "Aerodynamics of Wings with Elastically Produced Camber," MS Thesis, University of California, Davis, CA, Spring 1991.
12. Pickings, R.D., "Comparison of Theoretical Results with a Finite Element Model for Predicting Camber Induced by Bending of a Wing Box," MS Thesis, University of California, Davis, CA, Fall 1991.

TABLE 1.- CAMBER CORRELATION-METHOD 1

	<u>ANALYSIS</u>	<u>EXPERIMENT</u>
CAMBER COMPLIANCE (LB-IN ²) ⁻¹ × 10 ⁶	1.08	1.08
PERCENT DIFFERENCE	----	0.5

TABLE 2.- SPANWISE BENDING COMPLIANCE CORRELATION-METHOD 2

	ANALYSIS	EXPERIMENT
SPANWISE BENDING COMPLIANCE (LB-IN ²) ⁻¹ × 10 ⁶	0.78	0.85
PERCENT DIFFERENCE	----	9.0

TABLE 3.- CAMBER CORRELATION-METHOD 2

	<u>ANALYSIS</u>	<u>EXPERIMENT</u>
CAMBER COMPLIANCE (LB-IN ²) ⁻¹ × 10 ⁶	0.99	1.08
PERCENT DIFFERENCE	----	9.1

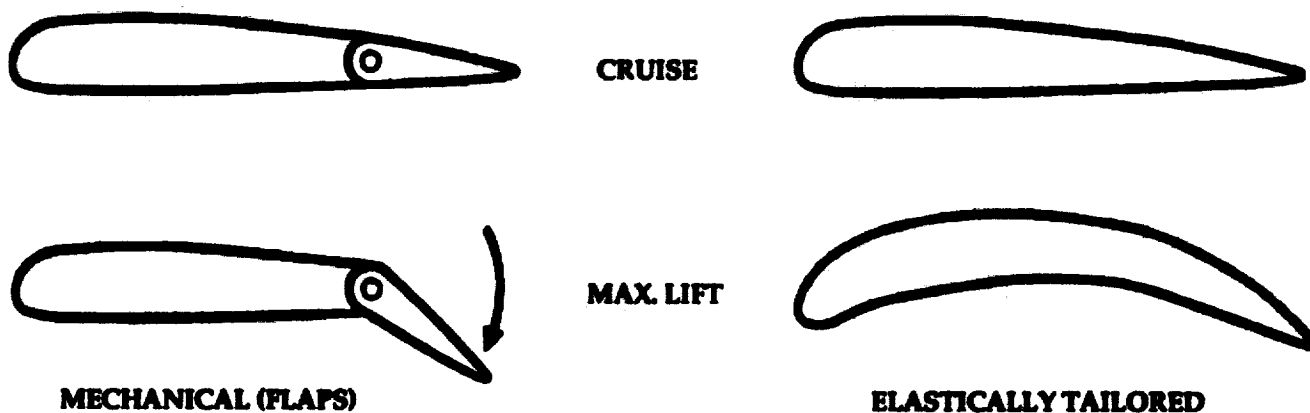


FIGURE 1. - METHODS OF INCREASING AIRFOIL LIFT

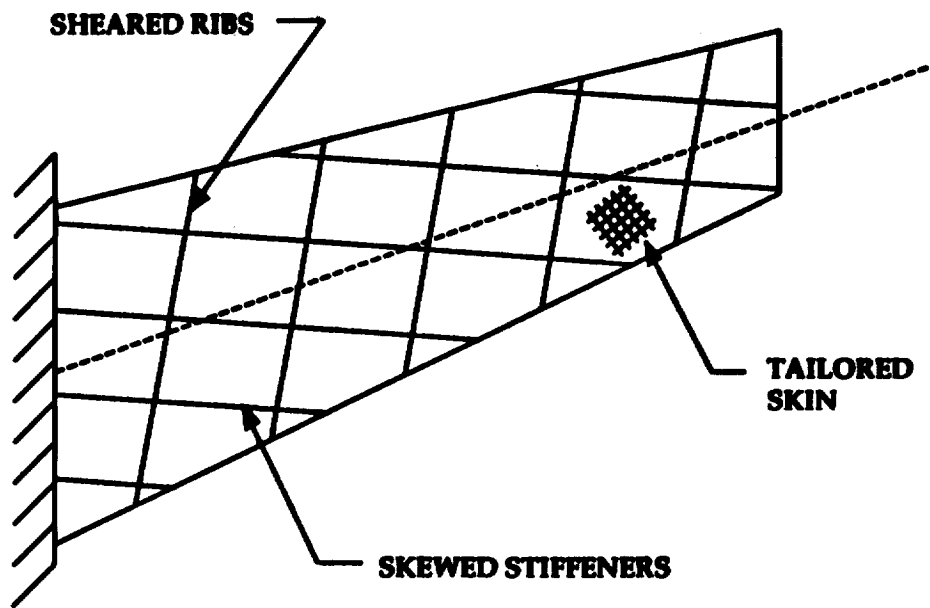


FIGURE 2. - METHODS FOR PRODUCING ELASTIC COUPLING IN HIGH ASPECT RATIO WINGS

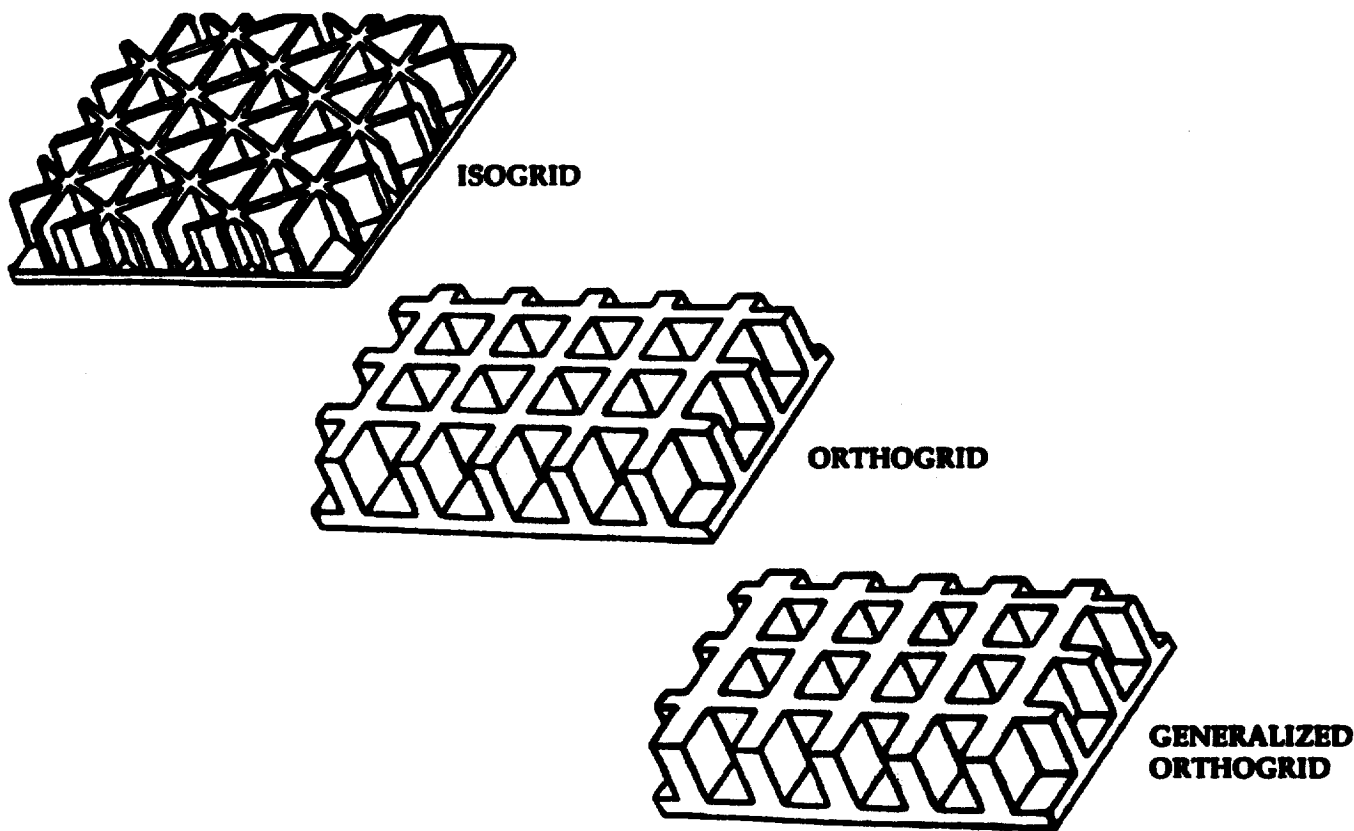


FIGURE 3. - GRID CONFIGURATIONS

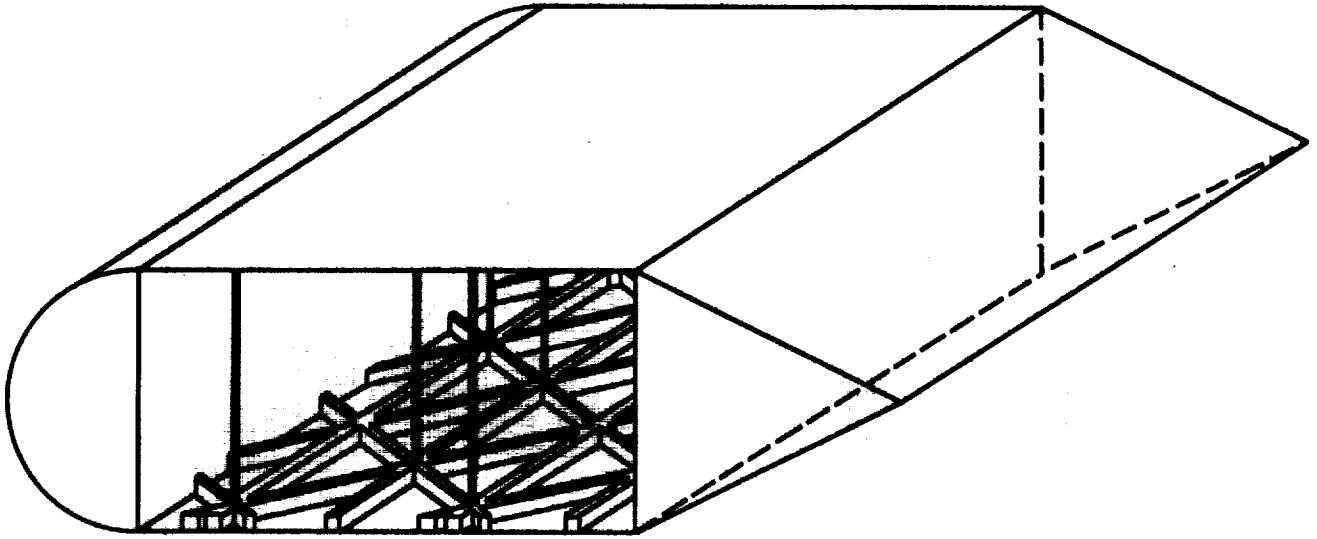


FIGURE 4. - VERTICAL COLUMN SUPPORT

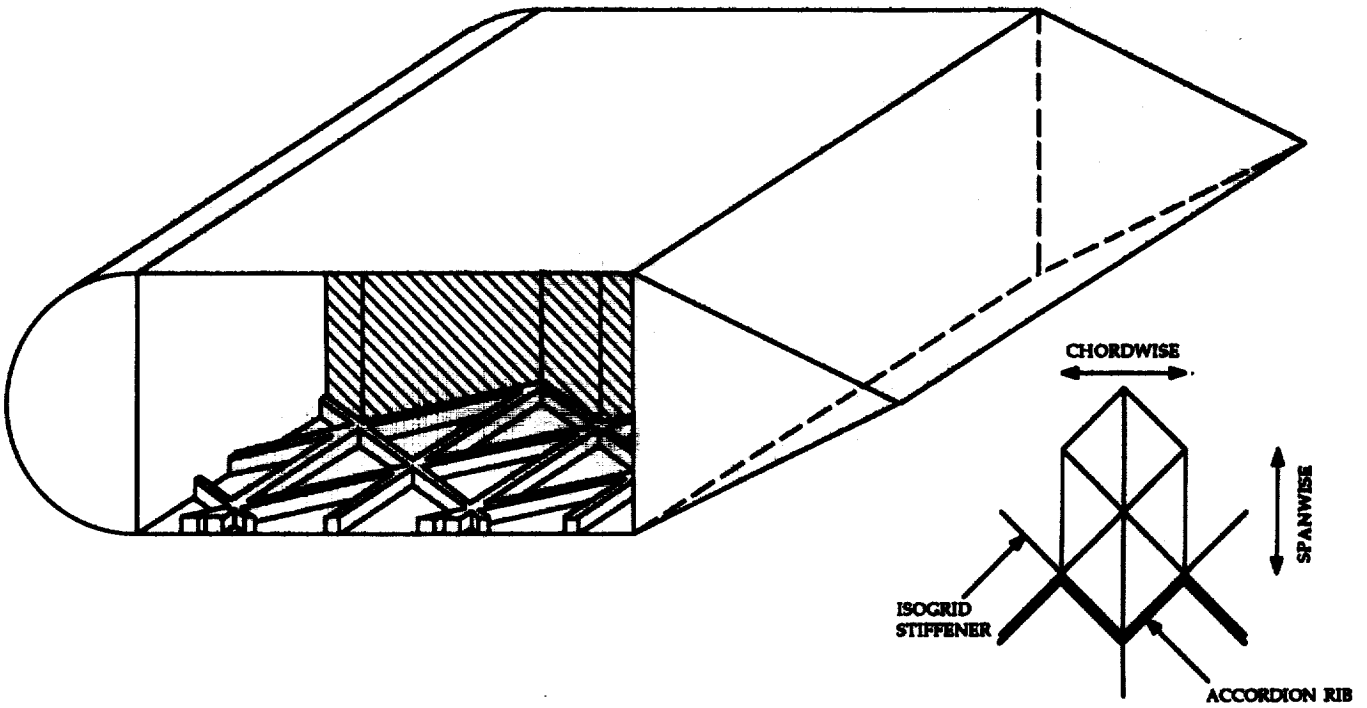


FIGURE 5. - ACCORDION RIB SUPPORT

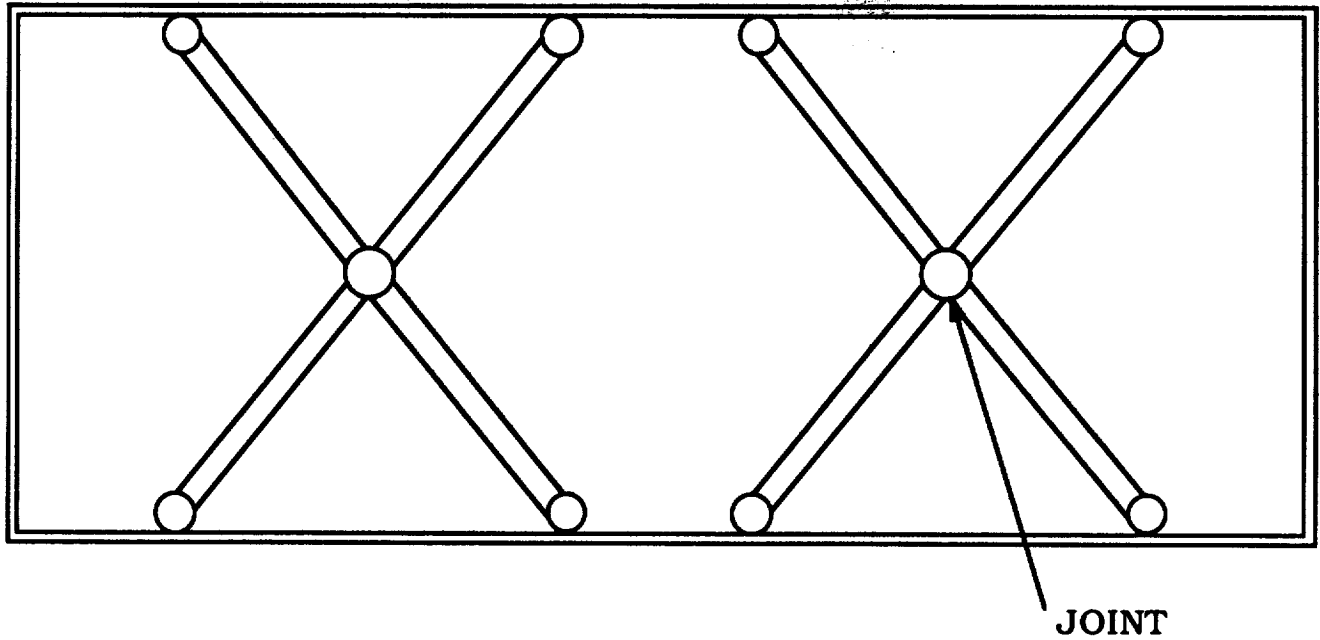


FIGURE 6. - SEGMENTED DIAGONAL COLUMNS WITH MIDSECTION JOINTS

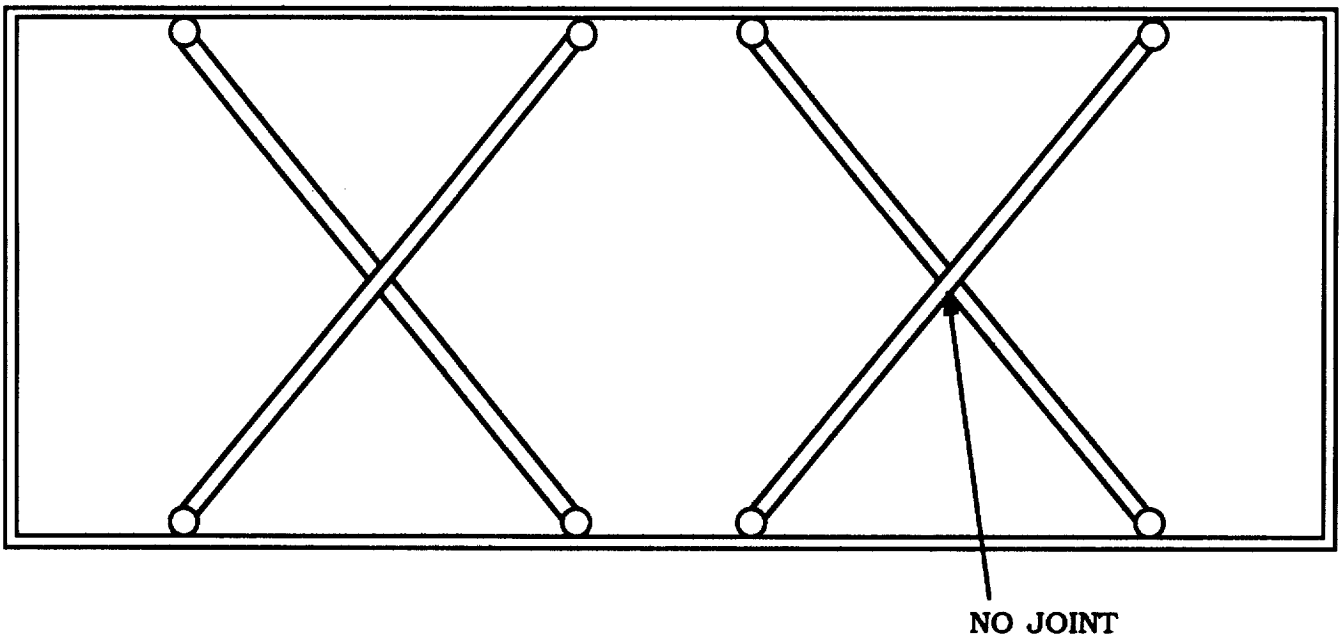


FIGURE 7. - SEGMENTED DIAGONAL SUPPORTS WITHOUT MIDSECTION JOINTS

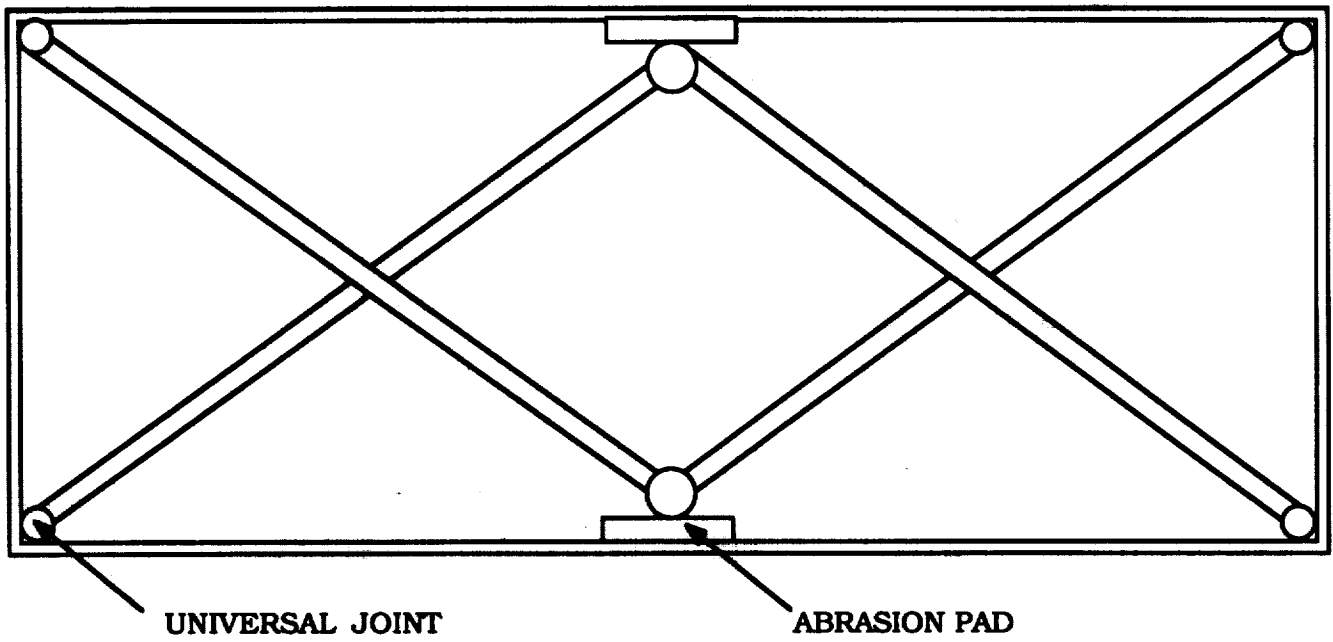


FIGURE 8. - FLOATING RIB STRUCTURE

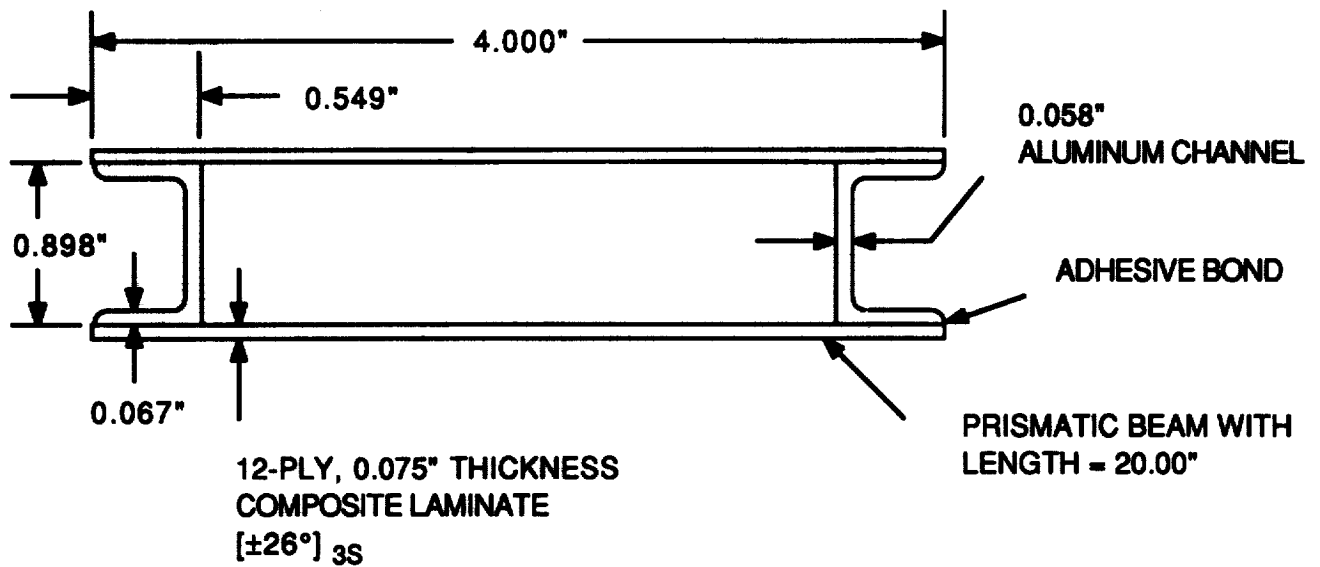


FIGURE 9. - BOX BEAM TEST SPECIMEN

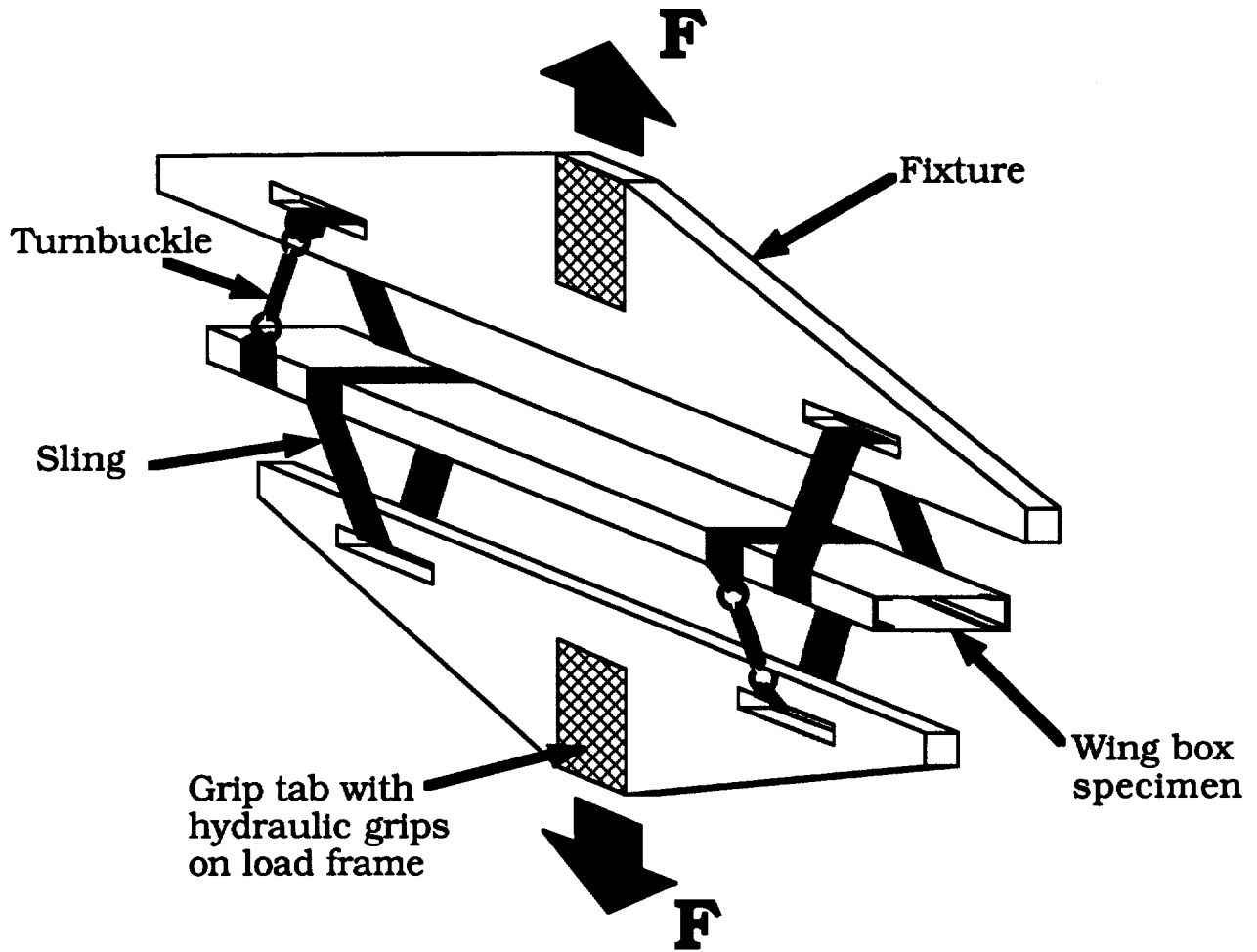


FIGURE 10. - OVERALL TEST CONFIGURATION

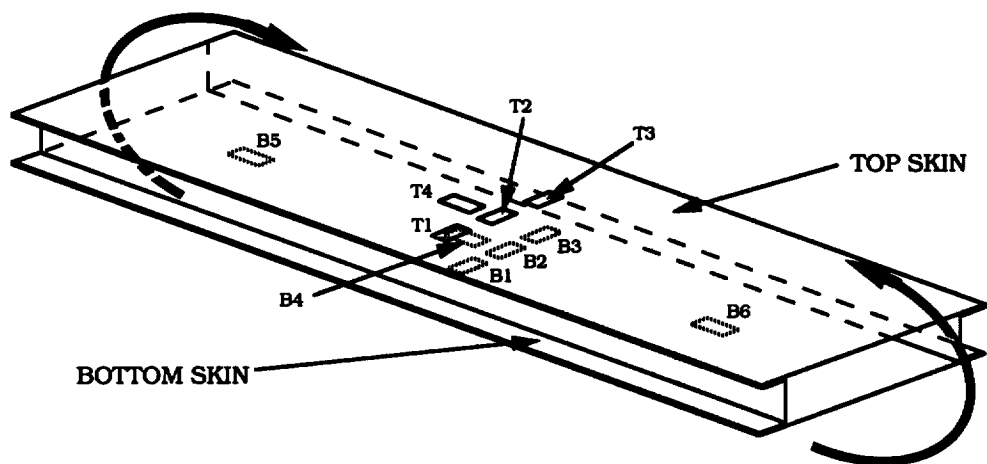


FIGURE 11. - STRAIN GAGE NOMENCLATURE AND LOCATIONS ON BOX BEAM

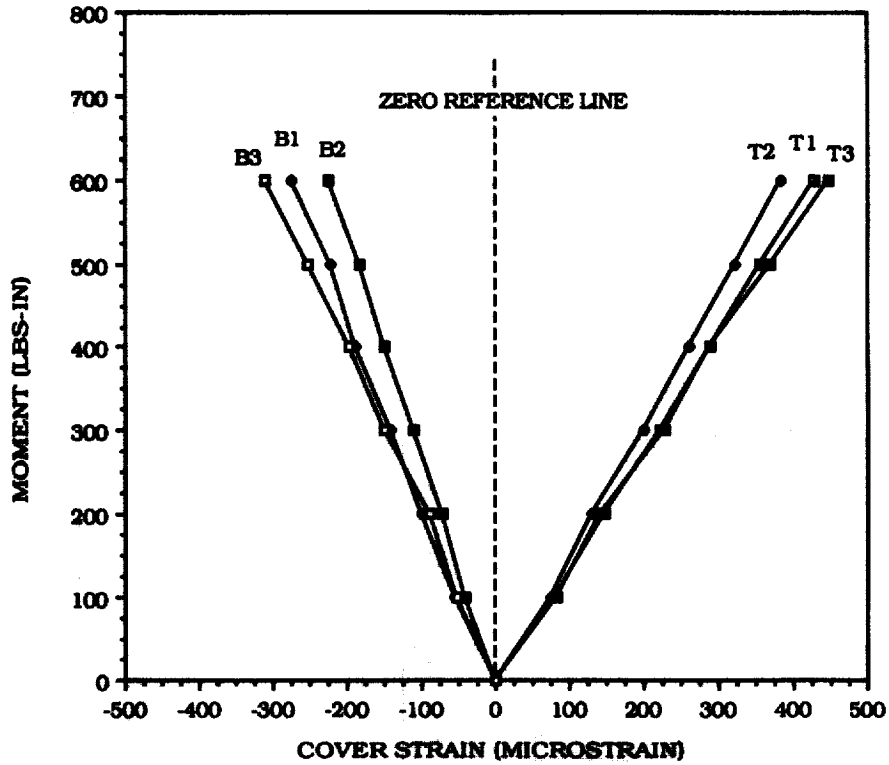


FIGURE 12. - BENDING MOMENT VS CHORDWISE GAGE STRAIN

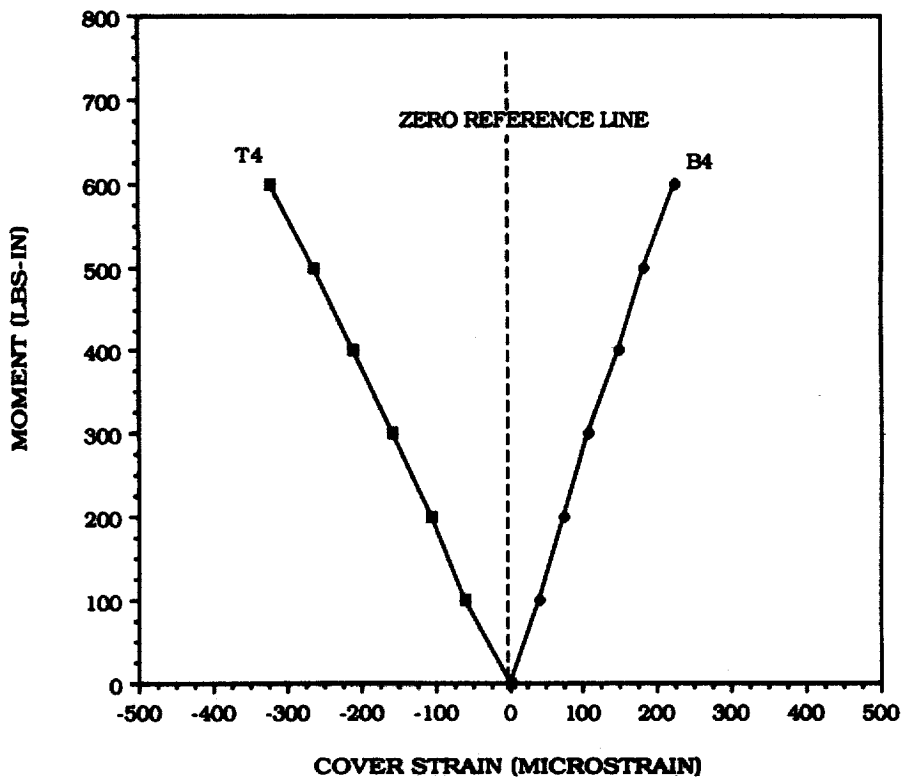


FIGURE 13. - BENDING MOMENT VS SPANWISE GAGE STRAIN

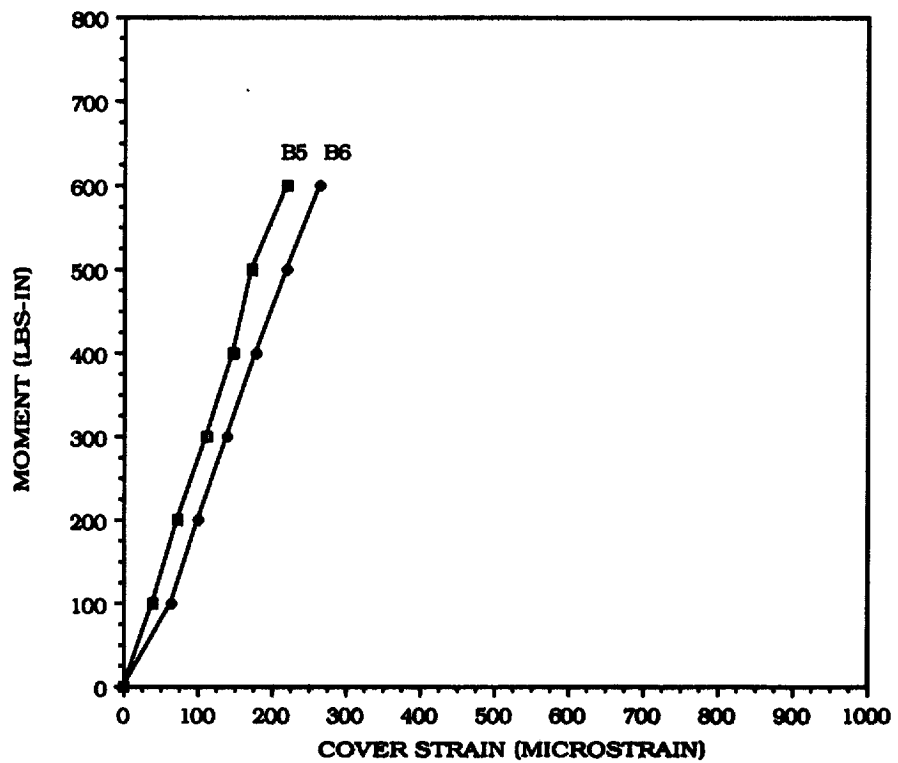


FIGURE 14. - BENDING MOMENT VS OUTER SPANWISE GAGE STRAIN

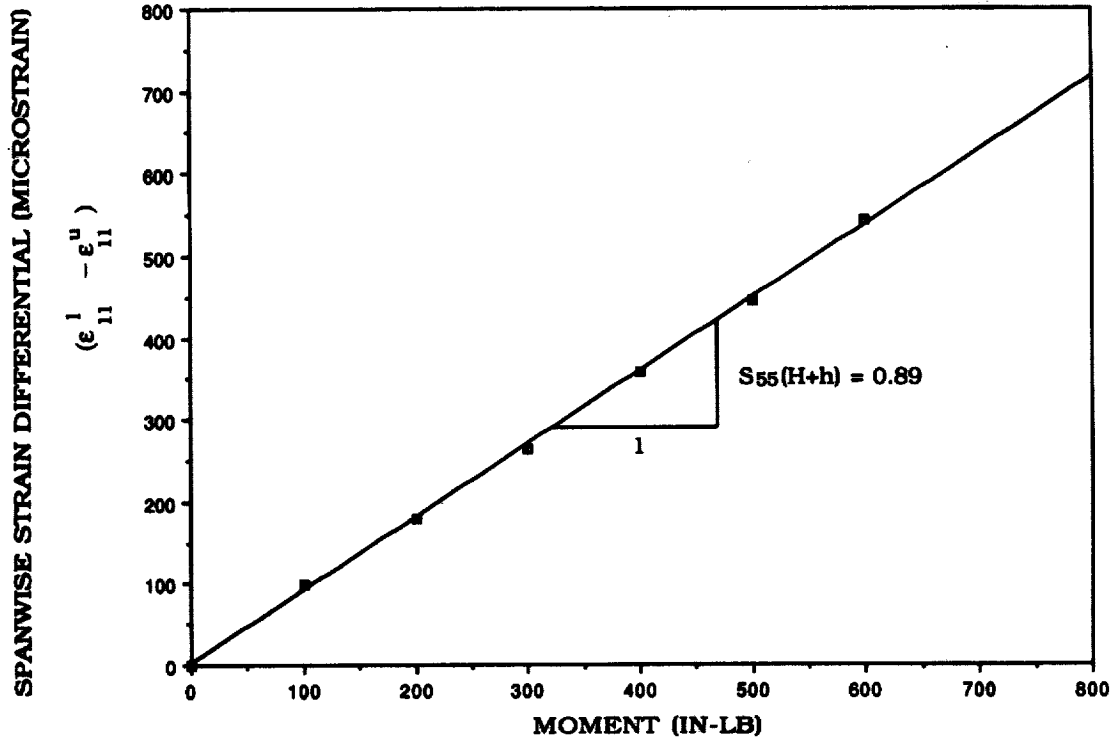


FIGURE 15. - SPANWISE STRAIN DIFFERENTIAL VS. APPLIED MOMENT

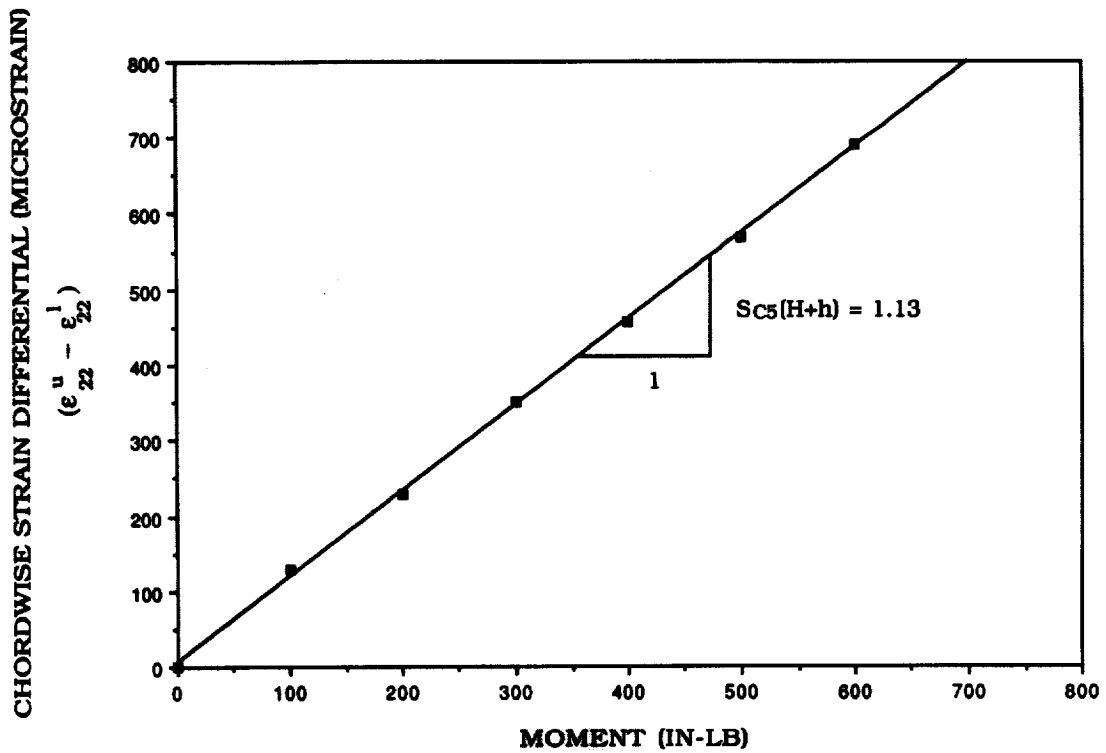


FIGURE 16. - CHORDWISE STRAIN DIFFERENTIAL VS. APPLIED MOMENT